Power Balance of Capacitive Wireless Power Transfer

Jan Kracek[#1], Milan Svanda[#2]

[#]Department of Electromagnetic Field, Faculty of Electrical Engineering, Czech Technical University in Prague, Czech Republic
{[1]jan.kracek, [2]milan.svanda}@fel.cvut.cz

***Abstract* — The power balance analysis of the capacitive wireless power transfer was conducted in a general manner. The circuit model of a capacitive wireless power transfer chain was presented. The derivation of the power transfer efficiency through the chain in question as well as the active power delivered to the appliance terminating this chain was shown. The case of the maximal efficiency was treated and conditions for this optimum were found. The appliance power corresponding to the maximal efficiency was also expressed. For the optimal conditions, the appliance power was written in the normalized form, which enabled to express it as a function of single variable in the same way as the efficiency.**

I. Introduction

The paper deals with a general rigorous circuit analysis of a power balance for a wireless power transfer (WPT) chain, which realizes the WPT with the help of capacitive coupling. The block scheme of the WPT chain, which is further detailed for the capacitive WPT (CWPT), is depicted in Fig. 1 [1]. There is a "wireless" transfer medium between the source side and appliance side. The power is transferred wirelessly through this medium from the source to the appliance. The medium is separated from both the source and appliance by adaptors that ensure an efficient transfer. The adaptors form electromagnetic field with the help of suitable coupling elements. In addition, they contain matching networks and typically also frequency converters because suitable frequencies for transfer through the medium differ from suitable frequencies for the source and appliance. In the case of the CWPT, the coupling elements are formed by a system of electrodes and the WPT is mediated just by the capacitive coupling of the electrodes.

The CWPT belongs to near field WPT technologies. The basic ideas of the near field WPT were presented by Nikola Tesla, who articulated the CWPT principles [2] as well as inductive WPT (IWPT) principles [3] more than hundred years ago. After a relatively long period of time, in 1960s, the IWPT was further evolved [4], [5], especially for medical implants, whereas the CWPT remained undeveloped. In 2010s, the WPT gained a new motivation in the massive expansion of personal portable appliances and sensor networks with low power consumption. Since then, the principles of the WPT have been revised and extensively investigated, which has led to development of both theory of the CWPT [6], [7] and IWPT [8], [9] and their different applications [10], [11] and [12], [13] respectively.

The analysis of the CWPT chain presented in this paper generalizes the results from [6], [7]. It is developed as the dual case to the analysis of the IWPT chain [8]. Its extension is treated in [14]. The paper structure is as follows: In Section II, the circuit model of the CWPT chain is described. In Section III, the derivation of the power transfer efficiency through the chain in question as well as the active power delivered to the appliance terminating this chain is shown. Further, the maximal efficiency as well as conditions for this maximum are found. In Section IV, the analysis is concluded.

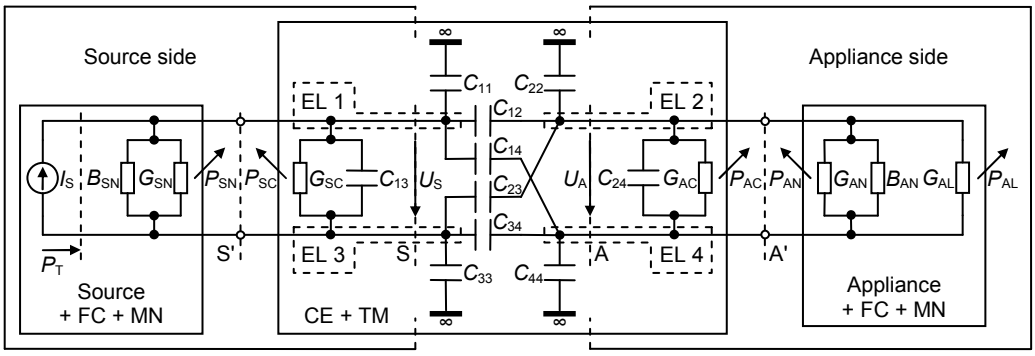

Fig. 1. Circuit model of CWPT chain (FC – Frequency Converter, MN – Matching Network, CE – Coupling Element, TM – Transfer Medium, EL – Electrode).

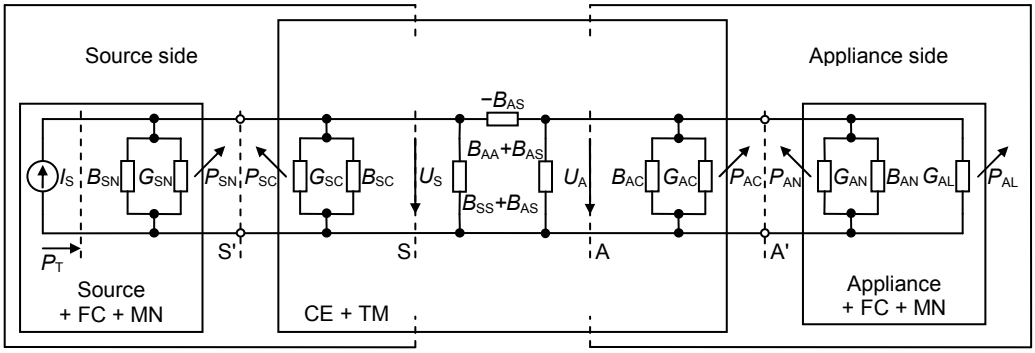

Fig. 2. Circuit model of CWPT chain with capacitances represented by susceptances (FC – Frequency Converter, MN – Matching Network, CE – Coupling Element, TM – Transfer Medium).

II. Circuit Model

The circuit model of the CWPT chain is depicted in Fig. 1. The source, frequency converter (FC) and matching network (MN) on the source side are considered as one block, i.e., the equivalent source. Similarly, the appliance, frequency convertor (FC) and matching network (MN) on the appliance side are regarded as one block as well, i.e., the equivalent load. Finally, the coupling elements (CE) and transfer medium (TM) are also viewed as one block. In other words, the fundamental block, which represents the essence of the transfer, is composed of the coupling elements and transfer medium. The rests of the source and appliance sides are connected to the block in question as the equivalent source and load respectively. In the presented model, two electrodes (EL 1, EL 3) connected to the source side and two electrodes (EL 2, EL 4) connected to the appliance side are regarded as the coupling elements. The symbols in Fig. 1 mean the following:

B_{AN} and G_{AN} the equivalent susceptance and conductance of the FC and MN on the appliance side,

B_{SN} and G_{SN} the equivalent susceptance and conductance of the source (including the FC and MN on the source side),

G_{AC} and G_{SC} the conductances between the electrodes 2-4 and 1-3,

G_{AL} the conductance of the appliance,

C_{11}, C_{22}, C_{33}, C_{44} the capacitances of the electrodes 1, 2, 3, 4 with respect to infinity,

C_{12}, C_{13}, C_{14}, C_{23}, C_{24}, C_{34} the capacitances between the electrodes 1-2, 1-3, 1-4, 2-3, 2-4, 3-4,

I_S the source current phasor (in rms scale),

U_A and U_S the appliance and source voltage phasors (in rms scale),

P_{AC}, P_{AN}, P_{SC}, P_{SN} the active powers lost in the conductances G_{AC}, G_{AN}, G_{SC}, G_{SN},

P_{AL} the active power delivered to the conductance G_{AL} of the appliance,

P_T the total active power supplied by the source.

The conductances G_{AC}, G_{AN}, G_{SC}, G_{SN} represent parasitic losses in the CWPT chain. Note that the losses caused by serial resistances of the electrodes 1, 2, 3, 4 are neglected, while the losses resulting from parallel conductances are considered merely between the electrodes 1-3 and 2-4 and they are included by the conductances G_{SC} and G_{AC}.

For the following derivation, the circuit model in Fig. 1 is replaced by the equivalent circuit model in Fig. 2. Here, the two-port of the capacitances with respect to infinity and mutual capacitances between the source and appliance sides is replaced by the equivalent two-port. The latter provides a suitable formalism to perform all further derivations in a general manner while considering all aforementioned capacitances. The equivalent two-port in Fig. 2 is formed by a Π network with susceptances $B_{AA} + B_{AS}$, $-B_{AS}$, $B_{SS} + B_{AS}$. The two-port is purely reactive since it consists of the capacitances that are related to their susceptances through the expression

$$B_{ij} = \omega C_{ij}, i \in \{1,2,3,4\}, j \in \{1,2,3,4\} \tag{1}$$

where ω is the angular frequency. For the expression of the susceptances B_{AA}, B_{AS}, B_{SS} with the help of the susceptances B_{ij}, $i \in \{1, 2, 3, 4\}$, $j \in \{1, 2, 3, 4\}$, see [14]. In addition, the capacitances C_{13}, C_{24} are designed by their susceptances B_{SC}, B_{AC}, see Fig. 2, that are related to the capacitances by the expressions

$$B_{AC} = \omega C_{24} \tag{2}$$

$$B_{SC} = \omega C_{13}\,. \tag{3}$$

The voltages U_A and U_S constitute the solution of the circuit equations system, which describes the model in Fig. 2,

$$\begin{bmatrix} I_S \\ 0 \end{bmatrix} = \begin{bmatrix} Y_S & \mathrm{j}B_{AS} \\ \mathrm{j}B_{AS} & Y_A + G_{AL} \end{bmatrix} \begin{bmatrix} U_S \\ U_A \end{bmatrix} \tag{4}$$

where Y_A, Y_S are the admittances with conductances G_A, G_S and susceptances B_A, B_S given by the relations

$$Y_A = \underbrace{G_{AC} + G_{AN}}_{G_A} + \mathrm{j}\underbrace{\left(B_{AC} + B_{AN} + B_{AA}\right)}_{B_A} = G_A + \mathrm{j}B_A \tag{5}$$

$$Y_S = \underbrace{G_{SC} + G_{SN}}_{G_S} + \mathrm{j}\underbrace{\left(B_{SC} + B_{SN} + B_{SS}\right)}_{B_S} = G_S + \mathrm{j}B_S\,. \tag{6}$$

Solving the system (4), the voltages U_A and U_S can be written as

$$U_{\mathrm{A}} = \frac{-\mathrm{j}B_{\mathrm{AS}}}{\left(Y_{\mathrm{A}} + G_{\mathrm{AL}}\right)Y_{\mathrm{S}} + B_{\mathrm{AS}}^2} I_{\mathrm{S}} \tag{7}$$

$$U_{\mathrm{S}} = \frac{Y_{\mathrm{A}} + G_{\mathrm{AL}}}{\left(Y_{\mathrm{A}} + G_{\mathrm{AL}}\right)Y_{\mathrm{S}} + B_{\mathrm{AS}}^2} I_{\mathrm{S}} . \tag{8}$$

III. Power Transfer Efficiency and Appliance Power

A. General Formulas

The power transfer efficiency η is defined by means of the active power P_{AL} delivered to the conductance G_{AL} of the appliance and the active powers P_{A}, P_{S} lost in the conductances G_{A}, G_{S}, whose sum equals to the total active power P_{T} supplied by the source. The powers P_{A}, P_{AL}, P_{S}, P_{T} are given by the relations

$$P_{\mathrm{A}} = G_{\mathrm{A}} \left|U_{\mathrm{A}}\right|^2 \tag{9}$$

$$P_{\mathrm{AL}} = G_{\mathrm{AL}} \left|U_{\mathrm{A}}\right|^2 \tag{10}$$

$$P_{\mathrm{S}} = G_{\mathrm{S}} \left|U_{\mathrm{S}}\right|^2 \tag{11}$$

$$P_{\mathrm{T}} = P_{\mathrm{A}} + P_{\mathrm{AL}} + P_{\mathrm{S}} . \tag{12}$$

The definition formula of the efficiency η can be then stated as

$$\eta = \frac{P_{\mathrm{AL}}}{P_{\mathrm{T}}} = \frac{P_{\mathrm{AL}}}{P_{\mathrm{A}} + P_{\mathrm{AL}} + P_{\mathrm{S}}} . \tag{13}$$

From (13) using (5)–(11), the efficiency η and powers P_{A}, P_{AL}, P_{S} can be expressed as

$$\eta = \frac{G_{\mathrm{AL}} B_{\mathrm{AS}}^2}{\left(\left(G_{\mathrm{A}} + G_{\mathrm{AL}}\right)^2 + B_{\mathrm{A}}^2\right)G_{\mathrm{S}} + \left(G_{\mathrm{A}} + G_{\mathrm{AL}}\right)B_{\mathrm{AS}}^2} \tag{14}$$

$$P_{\mathrm{A}} = \frac{G_{\mathrm{A}} B_{\mathrm{AS}}^2}{D_{\mathrm{P}}} \left|I_{\mathrm{S}}\right|^2 \tag{15}$$

$$P_{\mathrm{AL}} = \frac{G_{\mathrm{AL}} B_{\mathrm{AS}}^2}{D_{\mathrm{P}}} \left|I_{\mathrm{S}}\right|^2 \tag{16}$$

$$P_{\mathrm{S}} = \frac{\left(\left(G_{\mathrm{A}} + G_{\mathrm{AL}}\right)^2 + B_{\mathrm{A}}^2\right)G_{\mathrm{S}}}{D_{\mathrm{P}}} \left|I_{\mathrm{S}}\right|^2 \tag{17}$$

where

$$\begin{aligned} D_{\mathrm{P}} = {} & \left(\left(G_{\mathrm{A}} + G_{\mathrm{AL}}\right)^2 + B_{\mathrm{A}}^2\right)\left(G_{\mathrm{S}}^2 + B_{\mathrm{S}}^2\right) \\ & + 2\left(\left(G_{\mathrm{A}} + G_{\mathrm{AL}}\right)G_{\mathrm{S}} - B_{\mathrm{A}} B_{\mathrm{S}}\right)B_{\mathrm{AS}}^2 + B_{\mathrm{AS}}^4 . \end{aligned} \tag{18}$$

Further, the maximal efficiency η_{MAX} as well as conditions for its maximum are found.

B. Maximal Power Transfer Efficiency

The maximum of the efficiency η with respect to the conductance G_{AL} and susceptance B_{AN} can be found from the conditions

$$\frac{\partial \eta}{\partial G_{\mathrm{AL}}} = 0 \tag{19}$$

$$\frac{\partial \eta}{\partial B_{\mathrm{AN}}} = 0 . \tag{20}$$

Solving the system (19), (20) and through (5), (14), the optimal values $G_{\mathrm{AL,MAX}(\eta)}$ and $B_{\mathrm{AN,MAX}(\eta)}$ of the conductance G_{AL} and susceptance B_{AN} are equal to

$$G_{\mathrm{AL,MAX}(\eta)} = G_{\mathrm{A}} \sqrt{1 + \frac{B_{\mathrm{AS}}^2}{G_{\mathrm{A}} G_{\mathrm{S}}}} \tag{21}$$

$$B_{\mathrm{AN,MAX}(\eta)} = -B_{\mathrm{AA}} - B_{\mathrm{AC}} . \tag{22}$$

From (14), (16) using (5), (18), (21), (22), the maximal efficiency η_{MAX} and corresponding power $P_{\mathrm{AL,MAX}(\eta)}$ delivered to the conductance $G_{\mathrm{AL,MAX}(\eta)}$ can be written in the form

$$\eta_{\mathrm{MAX}} = \frac{\kappa^2}{\left(1 + \sqrt{1 + \kappa^2}\right)^2} \tag{23}$$

$$\begin{aligned} & P_{\mathrm{AL,MAX}(\eta)} = \\ & = \frac{4\kappa^2 \sqrt{1 + \kappa^2}}{\underbrace{\left(1 + \zeta^2\right)\left(1 + \sqrt{1 + \kappa^2}\right)^2 + 2\kappa^2\left(1 + \sqrt{1 + \kappa^2}\right) + \kappa^4}_{p_{\mathrm{AL,MAX}(\eta)}}} \frac{\left|I_{\mathrm{S}}\right|^2}{4G_{\mathrm{S}}} \\ & = p_{\mathrm{AL,MAX}(\eta)} \frac{\left|I_{\mathrm{S}}\right|^2}{4G_{\mathrm{S}}} \end{aligned} \tag{24}$$

where

$$\kappa = \frac{B_{\mathrm{AS}}}{\sqrt{G_{\mathrm{A}} G_{\mathrm{S}}}} \tag{25}$$

$$\zeta = \frac{B_{\mathrm{S}}}{G_{\mathrm{S}}} . \tag{26}$$

Thus, the efficiency η_{MAX} can be expressed as a function of single variable κ, see Fig. 3. The variable κ describes the mutual arrangement of coupling elements through the susceptance B_{AS} and losses on the appliance and source sides through the conductances G_{A} and G_{S} respectively. The power $P_{\mathrm{AL,MAX}(\eta)}$ can be written as a function of three variables κ, ζ, $|I_{\mathrm{S}}|^2/(4G_{\mathrm{S}})$. The term $|I_{\mathrm{S}}|^2/(4G_{\mathrm{S}})$ can be considered as a scale factor of the normalized active power $p_{\mathrm{AL,MAX}(\eta)}$.

Given (6), (14), (23)–(26), the efficiencies η and η_{MAX} are apparently independent of, whereas the power $P_{\mathrm{AL,MAX}(\eta)}$ through the variable ζ dependent on the susceptance B_{SN}. Consequently, the susceptance B_{SN} can be freely chosen without any impact on the efficiency η_{MAX}. It is useful to determine the susceptance B_{SN} for the maximal power $P_{\mathrm{AL,MAX}(\eta)}$ and it can be found using the condition

$$\frac{\partial P_{\mathrm{AL,MAX}(\eta)}}{\partial B_{\mathrm{SN}}} = 0 . \tag{27}$$

Solving (27) and through (6), (24), (26), the optimal value $B_{\mathrm{SN,MAX}(\eta)}$ of the susceptance B_{SN} amounts to

$$B_{\mathrm{SN,MAX}(\eta)} = -B_{\mathrm{SS}} - B_{\mathrm{SC}} \tag{28}$$

and the relation (24) expressing the power $P_{\mathrm{AL,MAX}(\eta)}$ can be reduced to

$$\begin{aligned} P_{\mathrm{AL,MAX}(\eta)} &= \underbrace{\frac{4\kappa^2\sqrt{1+\kappa^2}}{\left(1+\sqrt{1+\kappa^2}\right)^2 + 2\kappa^2\left(1+\sqrt{1+\kappa^2}\right)+\kappa^4}}_{p_{\mathrm{AL,MAX}(\eta)}} \frac{\left|I_{\mathrm{S}}\right|^2}{4G_{\mathrm{S}}} \\ &= p_{\mathrm{AL,MAX}(\eta)} \frac{\left|I_{\mathrm{S}}\right|^2}{4G_{\mathrm{S}}} \end{aligned} \tag{29}$$

which is a function of two variables κ, $|I_{\mathrm{S}}|^2/(4G_{\mathrm{S}})$. The normalized active power $p_{\mathrm{AL,MAX}(\eta)}$, which is a function of single variable κ, is depicted in Fig. 4.

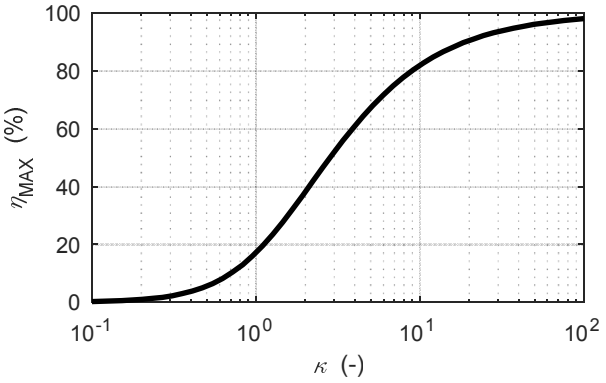

Fig. 3. Maximal power transfer efficiency.

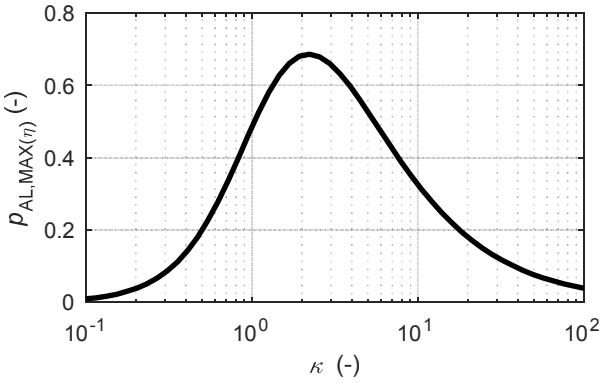

Fig. 4. Normalized active power delivered to appliance corresponding to maximal power transfer efficiency.

IV. Conclusion

The power balance analysis of the capacitive wireless power transfer was conducted in a general manner. The circuit model of a capacitive wireless power transfer chain was presented. The derivation of the power transfer efficiency through the chain in question as well as the active power delivered to the appliance terminating this chain was shown. The case of the maximal efficiency was treated and conditions for this optimum were found. The appliance power corresponding to the maximal efficiency was also expressed. For the optimal conditions, the appliance power was written in the normalized form, which enabled to express it as a function of single variable in the same way as the efficiency.

Acknowledgment

This work has received support from the Czech Science Foundation under the project GA17-02760S Wireless Sensing of Physical Quantities in Complex Environment.

References

[1] J. Kracek, M. Mazanek, "Wireless power transmission for power supply: State of art," *Radioengineering*, vol. 20, no. 2, pp. 457–463, Jun. 2011.

[2] System of transmission of electrical energy, by N. Tesla. (1900, Feb. 19). U.S. Patent 649 621.

[3] N. Tesla, "High frequency oscillators for electro-therapeutic and other purposes," *The Electrical Engineer*, vol. 26, no. 550, pp. 477–481, Nov. 1898.

[4] H. Stoeckle, J. C. Schuder, "Experimental experience with a micromodule pacemaker receiver sutured directly to the left ventricle," *Circulation*, vol. 27, no. 4, pp. 676–681, Apr. 1963, DOI: 10.1001/jama.1963.03700170128095.

[5] J. C. Schuder, H. E. Stephenson, Jr., "Energy transport to a coil which circumscribes a ferrite core and is implanted within the body," *IEEE Transactions on Biomedical Engineering*, vol. BME-12, no. 3–4, pp. 154–163, Jul.–Oct. 1965, DOI: 10.1109/TBME.1965.4502372.

[6] R. Dias Fernandes, J. N. Matos, N. Borges Carvalho, "Resonant electrical coupling: Circuit model and first experimental results," *IEEE Transactions on Microwave Theory and Techniques*, vol. 63, no. 9, pp. 2983–2990, Sep. 2015, DOI: 10.1109/TMTT.2015.2458323.

[7] B. Minnaert, N. Stevens, "Conjugate image theory applied on capacitive wireless power transfer," *Energies*, vol. 10, no. 1, Jan. 2017, DOI: 10.3390/en10010046.

[8] J. Kracek, M. Mazanek, "Power balance of inductive wireless power transmission," in *European Conference on Antennas and Propagation, EUCAP 2011*, Rome, Italy, 2011, pp. 3974–3978.

[9] M. Dionigi, M. Mongiardo, R. Perfetti, "Rigorous network and full-wave electromagnetic modeling of wireless power transfer links," *IEEE Transactions on Microwave Theory and Techniques*, vol. 63, no. 1, pp. 65–75, Jan. 2015, DOI: 10.1109/TMTT.2014.2376555.

[10] D. Ludois, J. Reed, K. Hanson, "Capacitive power transfer for rotor field current in synchronous machines," *IEEE Transactions on Power Electronics*, vol. 27, no. 11, pp. 4638–4645, Nov. 2012, DOI: 10.1109/TPEL.2012.2191160.

[11] K. Wang, S. Sanders, "Contactless USB – A capacitive power and bidirectional data transfer system," in *IEEE Applied Power Electronics Conference and Exposition – APEC*, Fort Worth, TX, USA, 2014, pp. 1342–1347, DOI: 10.1109/APEC.2014.6803481.

[12] N. Borges Carvalho et al., "Wireless power transmission: R&D activities within Europe," *IEEE Transactions on Microwave Theory and Techniques*, vol. 62, no. 4, pp. 1031–1045, Apr. 2014, DOI: 10.1109/TMTT.2014.2303420.

[13] N. Borges Carvalho et al., "Europe and the future for WPT," *IEEE Microwave Magazine*, vol. 18, no. 4, pp. 56–87, Jun. 2017, DOI: 10.1109/MMM.2017.2680078.

[14] J. Kracek, M. Svanda, "Analysis of capacitive wireless power transfer," *IEEE Access*, vol. 7, pp. 26678–26683, Mar. 2019, DOI: 10.1109/ACCESS.2018.2883712.